Current and Wave Measurements in Support of Shallow Water Environmental Modeling

James H. Churchill
Physical Oceanography
Woods Hole Oceanographic Institution
Woods Hole MA 02543 USA

Albert J. Williams 3rd
AOP&E
Woods Hole Oceanographic Institution
Woods Hole MA 02543 USA

Geoffrey W. Cowles
Dept. of Fisheries Oceanography, SMAST
U. Mass.-Dartmouth
New Bedford, MA 02744 USA

***Abstract*- In support of development and validation of a wave and current model for the coastal zone off Massachusetts in the United States of America, two deployments of a small tripod were made in 15m depth in Buzzards Bay. The tripod bore an upward looking Acoustic Doppler Current Profiler (ADCP) and, on one deployment, a Modular Acoustic Velocity Sensor (MAVS) current meter 1.5m above the bottom. From burst measurements acquired every two hours by these two instruments, a pattern of tidally and wind-driven flow with vertical shear was captured. Measurements of near-bottom current and wave orbital motion with MAVS extended the ADCP measurements from near the surface to the bottom region where interaction with the sediment is episodically important. In the September-October, 2008 deployment, the net flow north of Naushon Island was out of Buzzards Bay in alignment with the mean alongshore wind, which was mostly northeast (out of the bay) during this period. The water leaving the bay near Naushon Island must be made up somewhere else in the bay. Upwelling is also the dominate process north of Naushon Island, even when the winds measured at buoy BUZM3 at the SW opening of Buzzards Bay are near zero velocity. Waves are short period, typically broadband but with a peak near 5 seconds, fetch limited but still restricted to the along axis direction in Buzzards Bay. The longest fetch is in the ENE direction and the greatest wave event was from that direction with a significant wave height of 1.3m and frequency of 0.2Hz, from a 16m/s NE wind. When conditions were calm, a consistent swell from the southwest of 22cm significant wave height and 14s period could be observed propagating in from the open Atlantic at the mouth of Buzzards Bay.**

It is common for the wind to reverse direction diurnally and the waves respond quite quickly to these reversals from into the bay to out of the bay. Since this is a typical summer and early fall pattern, models must represent this rapid wave response to wind forcing. The delay between the maximum wind and the maximum waves is as little as 14 hours. Extreme winter conditions are dominated by NE cyclonic storms and a deployment January 20, 2009 captured such strong NE winds. NW winds were a winter addition to the fall pattern and there were no strong SW winds in winter. A preliminary model was applied to the fall data from the tripod.

In the coastal zone off Massachusetts, there is keen interest in power generation from wind turbines with our measurement site one of several under consideration. However, modeling of shallow-water, coastal response of current and wave to wind is useful for the other proposed sites as well as that north of Naushon Island. The development and validation of the model or models with these data will serve these alternate sites and should inform decision makers about environmental concerns at each site under consideration.

I. Introduction

Within the coastal zone influenced by wind and tide, current and wave response can be modeled. However, the models being developed must be tuned and validated with observations. Buzzards Bay in southern New England, between Cape Cod and the mainland of Massachusetts, serves as our observatory for development of these models. Buzzards Bay is open to the Atlantic Ocean to the southwest, extends 20 miles to the east north east, and has little input of water from sources other than the Atlantic Ocean. Cape Cod Canal at the upper end, Woods Hole passage, and several small rivers and marshes contribute small inputs but currents in the bay are dominated by wind and tidal forcing.

Our project is designed to model the wave and current regime in the coastal zone off Massachusetts, as this is critical for managing the region's productive ecosystem and assessing proposals for exploiting the region's resources. Traditionally, regional circulation models have not included the interplay between surface waves and currents. In the coastal zone, this can be a serious omission as surface waves have offsetting effects on underlying currents. At the sea surface, the increased roughness due to surface waves enhances the transfer of momentum from the wind to the ocean; whereas, at the seafloor, waves act to increase bottom stress and retard the overlying current. Ignoring wind/surface wave/ocean current interaction can be particularly serious in models directed at predicting storm surge run-up and coastal inundation.

Our study will produce a coupled surface wave-hydrodynamic model that has been refined and tested with field measurements. The model will be a robust tool that can be applied to a number of coastal management issues, including storm surge prediction, the impact of planned or natural inlet modification, and assessing the environment to which proposed coastal or offshore facilities will be exposed.

II. Instrumentation

A. Tripod

Wave and current measurements were made using a small tripod (Fig. 1) to support an Acoustic Doppler Current Profiler (ADCP) and Modular Acoustic Velocity Sensor (MAVS). Rigid sensor support for turbulence measurement dictates a bottom mount, either a piling or tripod. Keeping the tripod

Fig. 1. The small tripod supports a MAVS and an ADCP sensor for current, wave, and turbulence measurements. The ADCP is on the far footpad, the MAVS is mounted to the vertex, and two acoustic command releases, one horizontal on the near strut and the other vertical on the left diagonal can activate the pop-up floats each with a pair of orange balls and a lift line wrapped around its axle.

small and low reduces the overturning moment due to current [1]. Recovery of the tripod is accomplished by acoustic command release of pop-up floats [2] that carry a lifting line to the surface where it is captured, allowing the instrument to be winched aboard the recovery vessel. The MAVS current meter is mounted at the vertex to stay out of the wake of the pop-up floats. The ADCP is mounted on a footpad since the closest bin is above the disturbance of the floats.

B. Sensors

The ADCP is set with a 4-Hz sample rate to acquire currents every 0.4hr within 50-cm range bins. Waves were determined from the ADCP data using a 17 minute data burst acquired every 2 hours. Fig. 2 shows the ADCP head with an antifouling coating of Desitin™ zinc-oxide ointment on the transducers to inhibit barnacle settlement.

The MAVS [3] measures vector flow at a single point 166cm above bottom along with pressure at a height of 170cm above bottom. The sample rate is 4Hz in 17 minute bursts every 2 hours as with the ADCP. MAVS was not used in the second deployment but is scheduled to be included in a third deployment in September 2009.

III. CURRENT OBSERVATIONS

A. First Deployment – Fall 2008

The fall deployment was September 11 until October 21, 2008. The deployment location in 15-m depth is shown in Fig. 3. Buzzards Bay is bounded on the SE by Naushon Island

Fig. 2. The ADCP transducers are covered with Desitin™ to inhibit barnacle settlement.

and others of the Elizabeth Islands in the lower bay and by Cape Cod in the upper bay. It is bounded on the NW by the mainland of Massachusetts. The NE end is closed except for the Cape Cod Canal while the SW end is open to the Atlantic Ocean.

Summer winds are typically from the SW in the afternoon, changing in the fall to frequent NE winds and some nor'easter storms. During the fall 2008 deployment, the average wind was NE leading to the vertically averaged current from the ADCP of 2.6cm/s to the SW as shown in Fig. 4. The alongshore winds measured at buoy BUZM3 at the SW opening of Buzzards Bay are shown in the upper panel of Fig. 5. In the lower panel are the low-pass filtered alongshore velocities measured by the ADCP (blue lines showing deep velocities and green lines showing shallow velocities). The alongshore orientation has been set to align with the depth-averaged mean-flow shown in Fig. 4 (at 33.28° CCW of east).

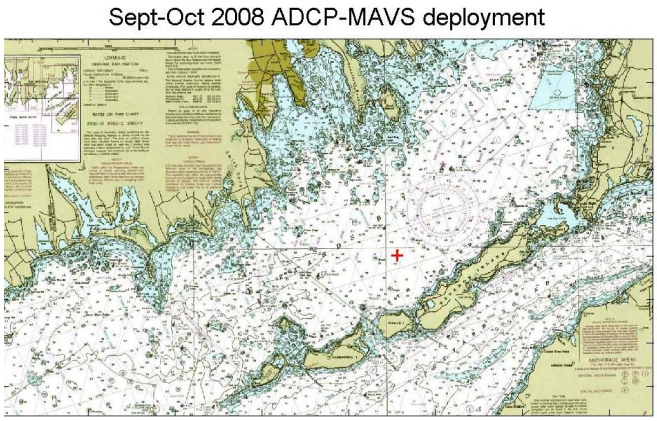

Fig. 3. The fall 2008 deployment in Buzzards Bay is indicated by the red cross in 15-m depth.

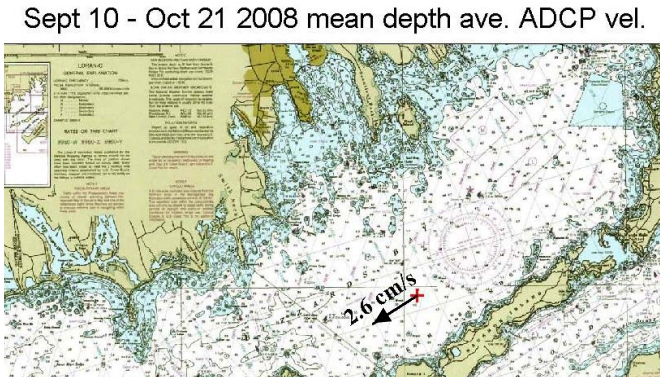

Fig. 4. The average current during the fall 2008 deployment was 2.6cm/s SW.

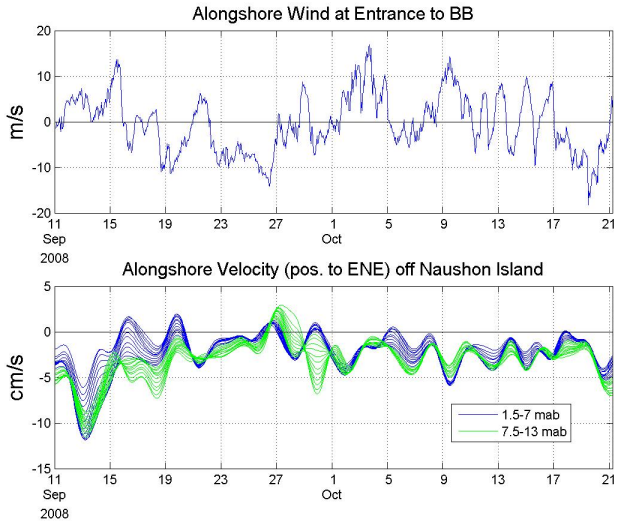

Fig. 5. Wind measured by buoy BUZM3 at the entrance to Buzzards Bay is shown in the top panel; current measured by the ADCP is in the lower panel.

Note that there is a fair amount of variation in the velocity signal, but this is not always clearly driven by the alongshore wind. There are additional complicated dynamics that we hope will be elucidated by the modeling. Also note that the mean out-of-bay alongshore flow persists throughout most of the record, even when the wind is directed up the bay (positive). This raises a question about how and where this flow is balanced by an incoming flow.

The across-shore velocity series shows a predominance of upwelling events, with the near-surface flow directed offshore and a compensating flow below (Fig. 6). These are not always tied to the alongshore wind in the manner prescribed by Ekman [4]. For the chosen coordinate system, a negative alongshore wind is upwelling favorable. While the negative alongshore winds of Sept. 19-26 correspond with persistent upwelling, upwelling is also seen when the BUZM3 alongshore winds are near zero or downwelling favorable. This is particularly evident during Oct. 13-17. It could be that the local alongshore wind differs from the BUZM3 wind. It is also possible that upwelling at our site is sometimes driven by an offshore-directed wind, a possibility considered in Fig. 7.

For those times when the upwelling shown by the ADCP velocities do not correspond with an upwelling-favorable alongshore wind at BUZM3 (e.g., 13-14 Sept. and 13-17 Oct.), the across-shore wind at the buoy is directed offshore – a possible cause for the upwelling at the site. It is also possible that downwelling is caused by onshore directed winds on September 15 and October 3-9.

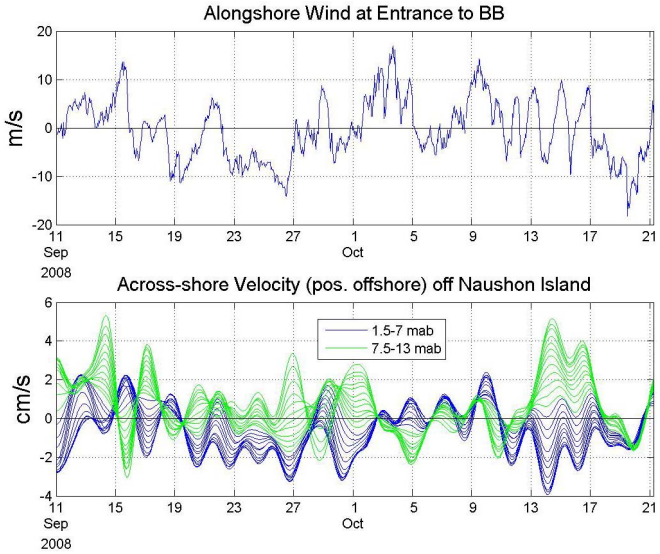

Fig. 6. Upwelling is shown in the profiles of the cross-shore flow in the lower panel. Upwelling is observed even when the alongshore wind is not upwelling favorable.

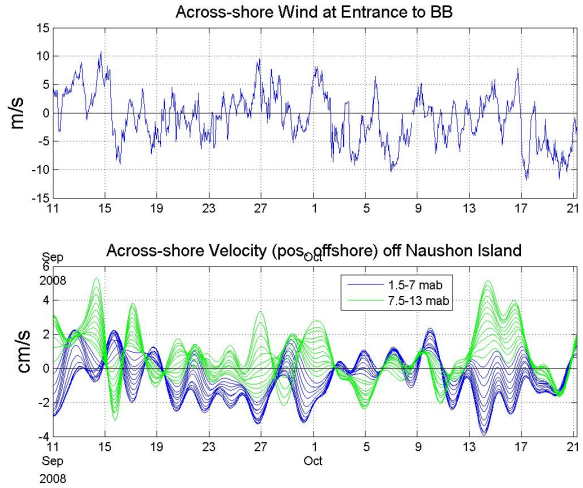

Fig. 7. Offshore winds may maintain upwelling even when alongshore winds are not favorable. Downwelling is forced by onshore winds on September 15 and October 3-9.

B. *Second Deployment – Winter 2009*

The winter deployment of the tripod, equipped as in the fall except that MAVS was not installed, lasted from January 20 to March 17. It was deployed at the same location in 15-m depth. Winter winds are rarely strong from the SW and are frequently strong from the NW, a direction rarely experienced in the summer and early fall. This appears to have had two effects on the winter currents. The first is a reduction of the SW mean current from 2.6cm/s to 1.3cm/s. The mean current is still out of the bay, in the SW direction, but reduced because of the predominant SW winds blowing to the NE (predominately SW but generally weak). See Fig. 8.

Upwelling and downwelling events occur with about equally frequency in the winter (Fig. 9). As in fall 2008, these are not always tied to the alongshore wind in the manner prescribed by Ekman [4]. In many instances, it seems to be the positive alongshore wind (downwelling favorable in the chosen coordinate system) that corresponds to upwelling (i.e., where the green lines in the series are positive). It is also notable that the strong upwelling favorable wind on March 1-2 corresponds to a nearly homogeneous across-shore current directed onshore. This is an example of a nor'easter, a typical winter storm [5].

As alongshore winds are not often responsible for driving upwelling/downwelling during the winter, the across-shore

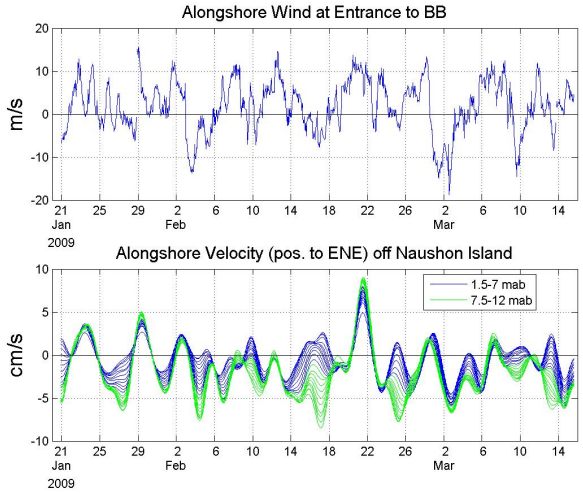

Fig. 8. Winter winds are predominantly from the SW although rarely strong from this direction. This reduces the average SW vertically-averaged current towards the SW to 1.3 cm/s.

winds must be more effective at doing so. Fig. 10 shows positive across-shore winds (directed offshore) that coincide with upwelling on January 28, February 11, 18, 27, and March 6-12. Downwelling on January 25, February 1, 6, 14, 25, and March 2-6 coincides with onshore winds. Unexplained events occur on February 15-19 (downwelling), and February 22,

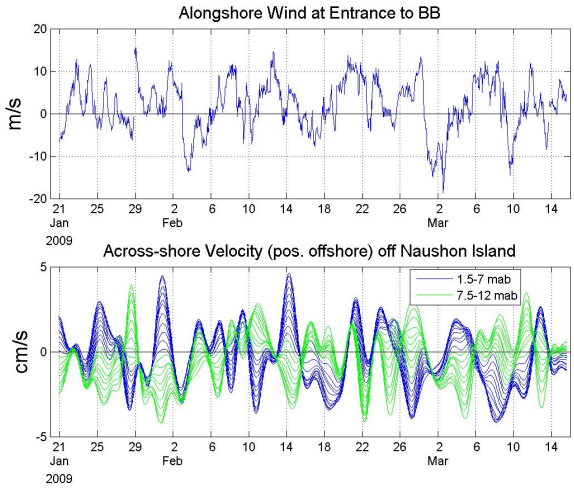

Fig. 9. Upwelling events are not always tied to alongshore upwelling wind direction. As many upwelling as downwelling events are seen in this winter record.

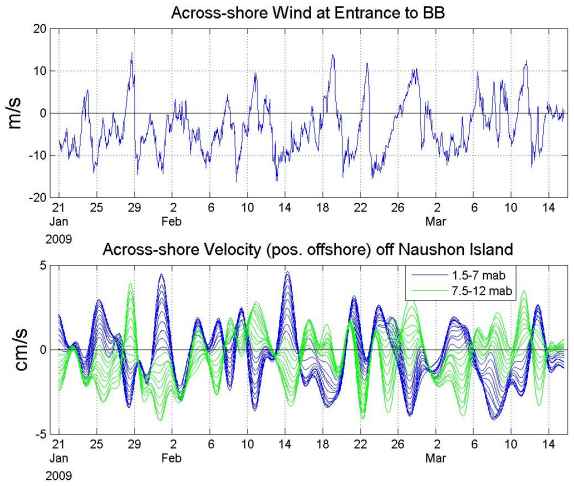

Fig. 10. The cross-shore wind seems to be of principal importance in driving the upwelling/downwelling off Naushon.

where the across-shore winds do not correspond to what is expected regarding upwelling/downwelling.

IV. WAVE OBSERVATIONS

A. *First Deployment – Fall 2008*

The significant wave height series, computed from the ADCP data, shows a number of events of elevated wave height. As seen in the contoured 1-D wave height spectra in Fig. 11, the waves of all events are relatively short, with periods generally less than 5s. For many events, the high

wave energy is spread out over a broad frequency band, indicating a complex sea.

The contoured 1-D spectra also frequently show a band of slightly elevated wave energy at low frequency, centered at around 0.1Hz. This could well be the signal of ocean swell that makes its way into Buzzards Bay. If so, this swell doesn't contribute much to the local wave field [6]. The significant

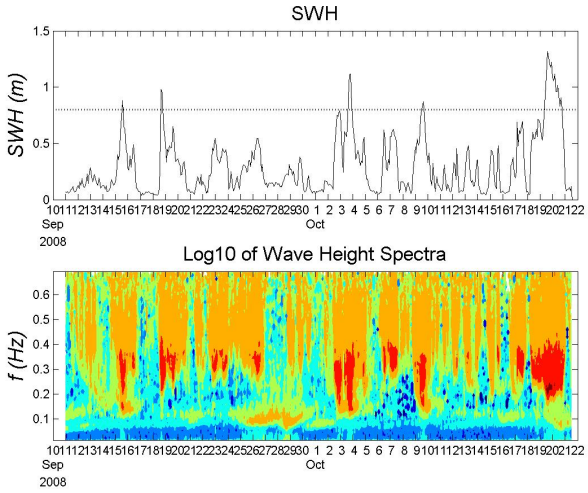

Fig. 11. Significant wave height (SWH) exceeds 0.8m five times during the fall deployment. Each has a spectral distribution of energy at periods shorter than 5s (0.2Hz). These are probably wind waves.

wave height determined when only the swell is present (Sept. 28) is no greater than 0.22m.

Fig. 12 compares wind speed to significant wave height and also suggests that the waves are wind waves. The SWH*15 in meters compares strongly with the wind speed in m/s.

Fig. 13, a scatter plot of winds showing the wave height for each wind direction and magnitude (via the color and size of each dot), indicates that high waves are associated with two wind direction bands. One is <u>to</u> (not from) the ENE, in the up

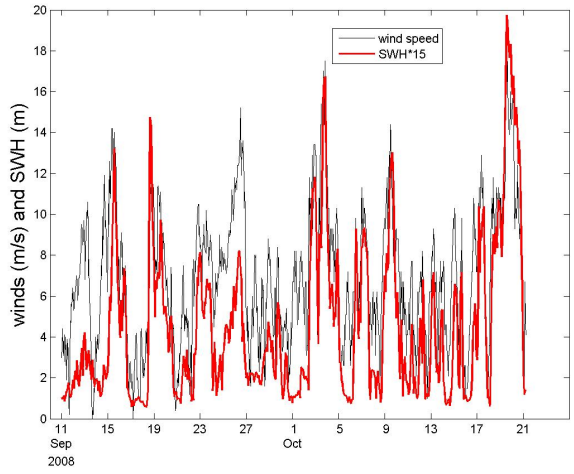

Fig. 12. Wind speed plots on top of SHW*15.

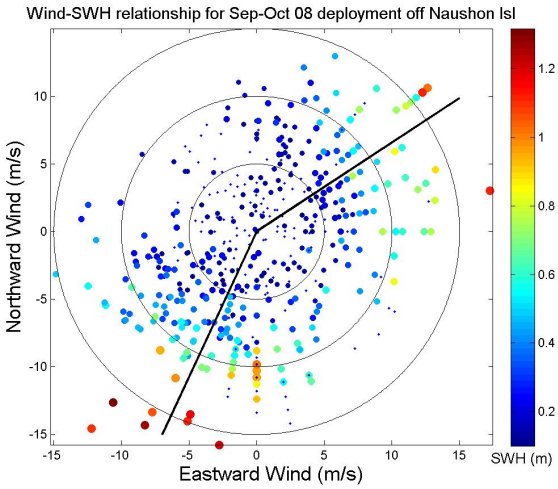

Fig. 13. The highest waves are generated from ENE winds that have the longest fetch. A secondary maximum SWH is in the NE direction from strong SW winds of early fall.

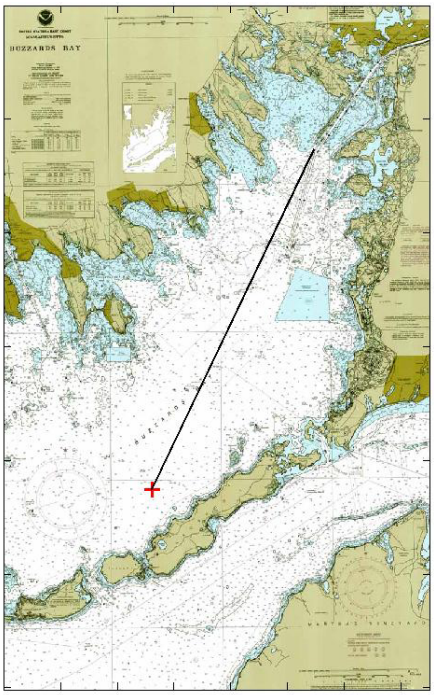

Fig. 14. The greatest wind and wave fetch inside Buzzards Bay is from the ENE.

bay direction. The other is to the SSW, down the bay, and is the wind band that actually encompasses the strongest waves. This is due to the fetch shown in Fig. 14.

B. *Second Deployment – Winter 2009*

In the fall, there were two wind directions that corresponded to high SWH. As indicated in Fig. 13, one was down the Buzzards Bay axis (to the SSW) and the other was coincident with the alongshore axis and to the NE. In the winter deployment, waves were still large when strong winds were directed down-bay, but the up-bay alongshore winds were never very strong and never produced large waves.

There was, however, another wind direction of high waves, from the NW. That this was not seen in the fall deployment is probably a simple result of the seasonally shifting wind regime in Buzzards Bay. In the fall deployment, winds from the NW were never in excess of 7m/s. This is illustrated in Fig. 15.

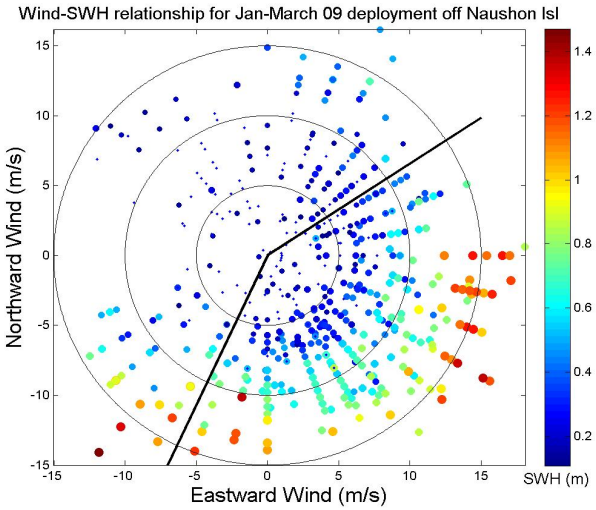

Fig. 15. In the winter, strong winds come from the NW although the strongest winds are the nor'easters from the ENE. There are no strong winds from the SW.

V. MODELING

The model system, to be tested and refined with examination of the data described above, will be formed by coupling two well tested numerical models: the Finite-Volume Coastal Ocean Model (FVCOM) [7] and the Surface WAves Nearshore (SWAN) model [8]. Developed at University of Massachusetts at Dartmouth, FVCOM solves a basic set of hydrodynamic equations on an unstructured grid and so is ideally suited for physically complex areas such as the Massachusetts coastal region. With MIT Sea Grant support, FVCOM has been used as the basis of an integrated model system for the Massachusetts coastal region (FVCOM-MC) with extremely high model resolution (grid spacing as small as 10m) in the near-shore region. SWAN is a phase-averaged wave model developed specifically for application in coastal waters.

The coupled FVCOM-MC/SWAN model system will account for the influx of wave momentum to the coastal zone, i.e., wave radiation stress, an important factor in generating near-shore currents and coastal sea level set up during storms. It will also include the effect of surface waves in modifying stress at the sea surface and seafloor. Using our collection of ocean current and surface wave data, we will work to refine the coupled model. Specifically, the observed current fields will be used to determine the optimal model vertical resolution, turbulence closure scheme and bottom friction parameterizations required for calculation of accurate near-bottom currents and bed friction in FVCOM. Wave spectra comparisons will be used to evaluate and improve the capability of the surface wave prediction component of FVCOM-MC (SWAN-UNS). We will determine the functional dependencies of growth and dissipation for best model-observation agreement and establish the optimal frequency of SWAN/FVCOM coupling.

Preliminary model runs have been conducted to determine the wave field for steady winds over Buzzards Bay. Runs were carried out for a number of wind speeds and directions. The resulting wave heights plotted as a function of wind speed and direction (Fig. 16) compare favorably in magnitude with the actual wave measurements shown in Figs. 13 and 15.

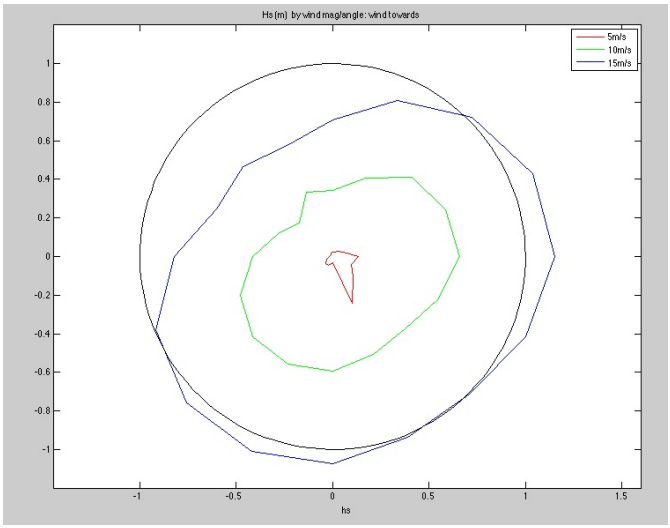

Fig. 16. A model of the SWH as a function of direction for three wind magnitudes is presented as a function of direction. It is similar to the observations shown in Figs. 13 and 15.

ACKNOWLEDGMENT

This work was supported by the Woods Hole Oceanographic Institution Sea Grant [9] and by the Woods Hole Oceanographic Institution.

REFERENCES

[1] Li, Weichang and A.J. Williams 3rd, (2006). "Cross-spectral phase method for distinguishing waves from turbulence in single-point boundary layer flow measurements," OCEANS 2006 Boston, 6 pages, ieeexplore.ieee.org/xpls/abs_all.jsp?arnumber=4098914.

[2] Williams, A.J.,3rd and A.T. Morrison III, (1996). "Shallow-Water Messenger-Line Recovery System", Oceans 96, pp. 646-649.

[3] Thwaites, F.T., and A.J. Williams 3rd, (1996). "Development of a Modular Acoustic Velocity Sensor", Oceans 96, pp. 607-612.

[4] Ekman, V.W., (1905). "On the influence of the earth's rotation on ocean currents", *Ark. Mat. Astron. Fys.*,**2:** 1-55.

[5] Williams, A. J. 3rd, A.T. Morrison III, and J.E. Farrell, Jr. (2007). "Measurements of surf zone currents and waves in support of Madaket and Sankaty Head, Nantucket, beach nourishment," OCEANS 2007 Aberdeen. ieeexplore.ieee.org/xpls/abs_all.jsp?arnumber=4302206.

[6] Williams, A.J. 3rd, and A.T. Morrison, III, (2005). "Near bottom measurement of wave environment in a tidal current," OEANS 2005 Brest, 6 pages, ieeexplore.ieee.org/xpls/abs_all.jsp?arnumber=1511768.

[7] Chen, C, R. C. Beardsley and G. Cowles, (2006). "An unstructured grid, finite-volume coastal ocean model (FVCOM) system." Special Issue entitled "Advances in Computational Oceanography", Oceanography, 19(1), 78-89.

[8] Booij, N., R.C. Ris, and L.H. Holthuijsen (1999). A third-generation wave model for coastal regions, Part I, Model description and validation, Journal of Geophysical Research, 104, 7649-7666.

[9] Churchill, J., A. Williams, and G. Cowles, (2008). "A measurement and modeling study of waves and currents in the coastal zone off southeastern Massachusetts," WHOI Sea Grant project, http://www.smast.umassd.edu/CMMS/Site/WHOI_SeaGrant.html